# Linear modeling of elongated bending EAP actuator at large deformations

Indrek Must[a], Mart Anton[ab], Maarja Kruusmaa[ac], Alvo Aabloo[a]
[a] IMS Lab, Institute of Technology, Tartu University, Nooruse 1, 50411 Tartu, Estonia
[b]Department of Electrical & Computer Engineering,
Michigan State University, East Lansing, MI 48824, USA
[c]Center for Biorobotics, Tallinn University of Technology,
Akadeemia tee 15A, 12618 Tallinn, Estonia

## ABSTRACT

This paper describes a linear dynamic model of an elongated bending Electroactive Polymer (EAP) actuator applicable with deformations of any magnitude. The model formulates relation of a) voltage applied to the EAP sheet, b) current passing through the EAP sheet, c) force applied by the actuator and d) deformation of the actuator. In this model only the geometry of EAP piece and four empirical parameters of the EAP material: a) bending stiffness, b) electromechanical coupling term, c) electrical impedance and d) initial curvature are considered. The contribution of this paper is introducing a model that can be used to characterize the properties of different EAP materials and compare them. The advantage of the model is its simplicity and ability to provide insights in to the behavior of bending EAPs. Additionally, due to linearity of the model, the real-time control is feasible. Experiments, using Ionomeric Polymer-Metal Composite (IPMC) sheet from Environmental Robotics Inc., where carried out to verify the model. The experimental results confirm the model is valid.

**Keywords:** EAP, IPMC, ICPF, modeling, characterization, linear, dynamic, large deformations

## 1. INTRODUCTION

Bending Electroactive Polymers (EAP) are materials that are able to bend in response to electric stimulation and vice-versa [1]. Because of their unique shape, large deformation, and the simple construction, they offer new opportunities for designing devices [2-5]. There are many types of EAP materials with different properties. Different applications have different requirements. To compare EAP materials and choose the one best suited for given application we need a scalable model of an EAP sensor/actuator, where the behavior of different EAP materials with specific mechanical construction and actuation mechanism would be defined in the same terms.

The need of unified characterization and modeling techniques has been recognized before and some steps have been taken in that direction [6], [7]. However, no scalable general purpose model has been presented so far.

Several researchers have worked on finding dynamic scalable models for different specific EAP materials [8], [9]. However, these models do not consider large deformations. We consider deformation of EAP sheet large, if the deflection angle is greater than 90 degrees. A large deformation model is presented in [10], [11]. These models are static and nonlinear. To the best of our knowledge, no linear, dynamic, and large deformation model has been presented so far.

In this paper linear, dynamic, large deformation universal model of an EAP actuator is presented. The actuator consists of EAP sheet and a rigid elongation attached on top of it. The advantages of using elongation are listed in [11], [12]. The model considers initial curvature of EAP and enables concurrently varying load and position. We characterize a sample of IPMC and use the model to estimate the behavior of that sample.

## 2. THE PROPERTIES OF EAP MATERIAL

There are many different types of EAP actuators with different construction and actuation mechanisms [1]. In this section four empirical parameters are introduced, which can describe the behavior of EAP material. The parameters are independent from the geometry of the actuator.

### 2.1 Normalized bending stiffness

All EAP sheets bend in response to applied force moment. Lets denote change in curvature with $\Delta k$ and bending moment with $M$. A bending stiffness is defined as $\frac{M}{\Delta k}$. The bending moment is proportional to the width of the sheet $w$. In this paper, the bending stiffness is normalized with the width to describe the EAP material and is defined as

$$\bar{B} = \frac{M}{\Delta k \cdot w}. \tag{1}$$

In the case of homogeneous material with Young modulus $E$ and thickness $d$, the normalized bending stiffness can be calculated from (2). An EAP actuator is usually made from a composite material. Even though, the material is not homogeneous it can still be treated using (2), where $E$ is the equivalent or effective Young modulus.

$$\bar{B} = \frac{E \cdot d^3}{12} \tag{2}$$

EAP-s can also have viscoelastic properties. The viscoleastic properties of Conductive Polymers (CP) is addressed in [9], [13].The viscoelastic properties of IPMC-s have been studied in [14], [15]. To account with viscoelasticity normalized bending stiffness can be a function of frequency. $M$ and $\Delta k$ may be then looked at as phasors in complex form.

### 2.2 Normalized electromechanical coupling

Although the actuation mechanisms of different EAP materials has dispersed physico-chemical background, applied voltage generates a bending moment in the material. There are different models developed for CP-based actuators [16] and IPMC-s [8, 17] We consider electrically induced bending moment $M_e$ to be proportional to the input voltage $U$. It is reasonable to assume that $M_e$ is proportional to the width of the sheet $w$. The normalized electromechanical coupling $\bar{K}$ is defined as

$$\bar{K} = \frac{M_e}{U \cdot w} \tag{3}$$

Electrically induced bending moment my be frequency dependant [8], [9]. Therefore, normalized electromechanical coupling is a function of frequency.

### 2.3 Normalized electrical impedance

We simplify the model, so that the current $I(s)$ through the material is proportional to the voltage $U(s)$, where $s$ is complex frequency. It is reasonable to assume that $I(s)$ is inverse proportional to the area $A$ of the sheet. The normalized electrical impedance is defined as

$$\bar{Z}(s) = \frac{U(s) \cdot A}{I(s)} \tag{4}$$

The normalized electrical impedance is related to effective impeditivity $X(s)$ of the material with thickness $d$ as follows:

$$\bar{Z}(s) = \frac{X(s)}{d} \tag{5}$$

### 2.4 Initial curvature

An EAP sheet may have an initial curvature. This can be caused by non-symmetrical manufacturing or treatment. Ionic EAP-s may also have hysteresis because they contain one or more layers of porous materials [18]. The hysteresis in IPMCs is studied in [19], [20].

## 3. THE MODEL

In this section we present a model to describe a bending EAP actuator.

### 3.1 The actuator

The actuator consists of a rectangular piece of EAP sheet in cantilever configuration. One end of the EAP sheet is clamped and a rigid elongation is attached to the other end (see Fig. 1). The rest of the EAP sheet can bend while a voltage is applied through clamps. No inertial nor friction forces are considered in our model.

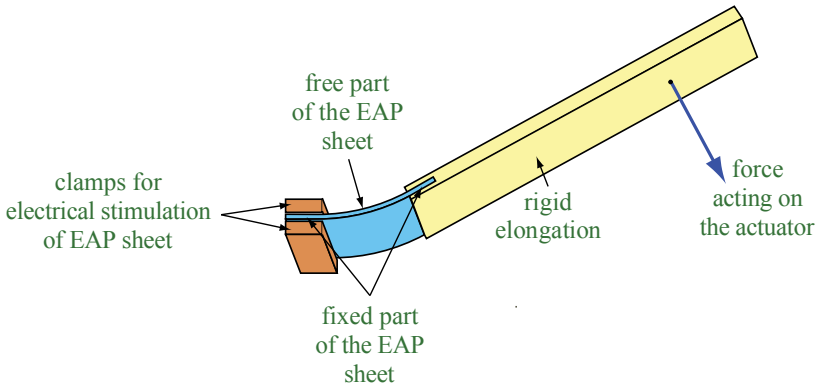


Fig. 1. Perspective view of the system.

### 3.2 Formulation of the task

Our model will formulate the relation of:

1) voltage applied to the EAP sheet,
2) current passing through the EAP sheet,
3) force applied by the actuator to resist the outer force acting on the actuator and
4) deformation of the actuator.

The model also considers the geometry of the actuator and properties of the EAP material as discussed in the previous section. Please refer to Table 1 for notations for the parameters.

We denote force applied by the actuator $F(s)$. A force $-F(s)$ is applied to the actuator at a fixed distance from a point located in front of the contacts. The point is called "joint of the EAP sheet" and would be exactly in the middle of the free part of the EAP sheet in case of a straight sheet (See Fig. 2). The line segment between this point and the point where the force is applied to is called arm of the actuator. The length of the arm is denoted as $R$. The deformation of the actuator is defined by the angular deflection of the arm. The force applied by the actuator (force output) $F(s)$ is always perpendicular to the arm.

Table 1. Notations of the model parameters.

| Type | Meaning | Notation | Unit |
|---|---|---|---|
| Dimensions of the EAP Actuator | Length of free part of the EAP sheet | $l$ | m |
| | Total length of the fixed part of the EAP sheet | $l_c$ | m |
| | Width of the EAP sheet | $w$ | m |
| | Arm length of the actuator | $R$ | m |
| The parameters of EAP material | Normalized bending stiffness of EAP | $\bar{B}(s)$ | $\mathrm{N\cdot m}$ |
| | Normalized electromechanical coupling of EAP | $\bar{K}(s)$ | $\mathrm{N\cdot V^{-1}}$ |
| | Normalized electrical impedance of EAP | $\bar{Z}(s)$ | $\Omega\cdot\mathrm{m^2}$ |
| | Initial curvature of EAP | $k_0$ | $\mathrm{m^{-1}}$ |
| Signals in frequency Domain | Angular deflection of the arm | $\alpha(s)$ | rad |
| | Voltage applied to the EAP sheet | $U(s)$ | V |
| | Force output of the actuator | $F(s)$ | N |
| | Electric current passing through the EAP sheet | $I(s)$ | A |

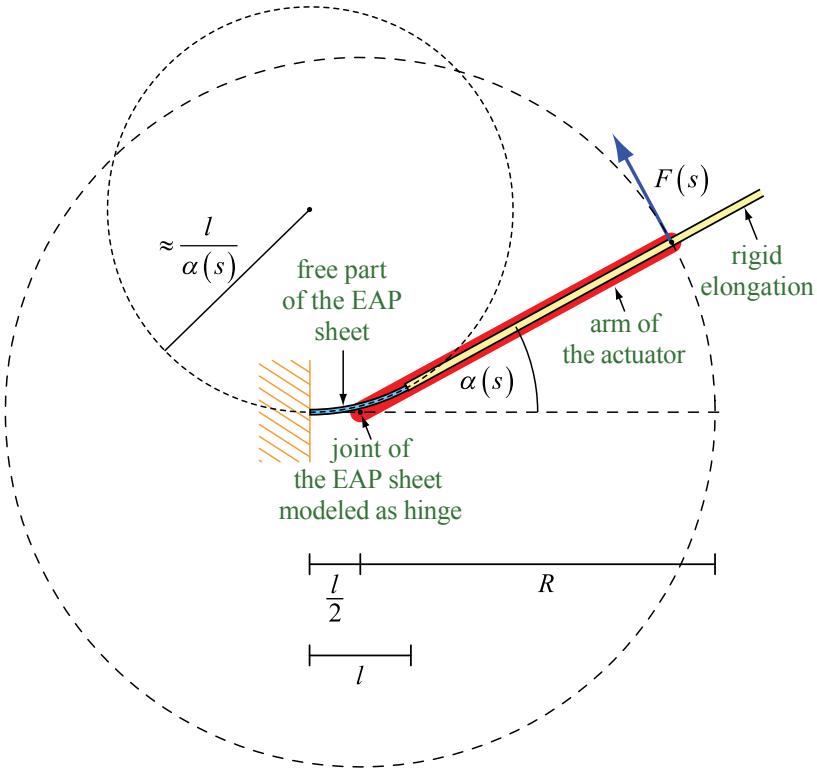


Fig. 2. The geometric definition of parameters. This is the top view of the system. Please consider that the elongation is close to but not strictly parallel to the arm.

In our model, we assume that the bending moment generated by the outer force, curvature, and all four parameters of the free part of EAP sheet are uniform. In [21] it is shown, that IPMC actuator can be modeled as a hinge with joint in the middle. The error of such approximation is calculated. The results can be easily extended to other bending EAP materials. Based on that we may assume, that the radius of curvature of EAP sheet can be approximated as $\frac{l}{\alpha(s)}$.

### 3.3 Solution

In [11] it is shown that the mean bending moment caused by an external force is equal to the bending moment in the center of the bendable section. That bending moment is approximately $-R \cdot F(s)$. This gives us the opportunity to utilize the theory in [11] for IPMC actuators with constant EIBM, which leads to the derivation of (6).

$$U(s) \cdot \bar{K}(s) = \left( \frac{\alpha(s)}{l} - \frac{k_0}{s} \right) \bar{B}(s) + F(s) \frac{R}{w} \tag{6}$$

From (4) and taking into account that area of the sheet is $A = w \cdot (l + l_c)$ we get the electrical model of EAP actuator

$$\frac{I(s)}{w \cdot (l + l_c)} = \frac{U(s)}{\bar{Z}(s)} \tag{7}$$

### 3.4 Inferences

From (6) $F(s)$ and $\alpha(s)$ can be revealed.

$$F(s) = \frac{w}{R} \left( U(s) \cdot \bar{K}(s) - \left( \frac{\alpha(s)}{l} - \frac{k_0}{s} \right) \bar{B}(s) \right). \tag{8}$$

$$\alpha(s) = \frac{l}{\bar{B}(s)} \left( U(s) \cdot \bar{K}(s) - F(s) \frac{R}{w} \right) + \frac{k_0}{s} \tag{9}$$

From (7) $I(s)$ and $U(s)$ can be revealed.

$$I(s) = \frac{U(s) \cdot w \cdot (l + l_c)}{\bar{Z}(s)} \tag{10}$$

$$U(s) = \frac{I(s) \cdot \bar{Z}(s)}{w \cdot (l + l_c)} \tag{11}$$

# 4. THE EXPERIMENTS

In this section the system setup for the experiments is presented and details of implementation are discussed.

## 4.1 Experimental device

The experimental device consists of a rigid clamp with electrical contacts made of gold attached to an EAP test sample (See Fig. 3). A light-weight rigid elongation made of PC and carbon fiber is attached to the opposite end of sample. The free length of the sample can be freely adjusted by varying a length of EAP between the securing plates on the elongation. An isometric transducer MLT0202 from AD instruments is softly attached to the elongation at a desired distance. The strain is measured approximately perpendicular to the arm (and to the elongation) of the actuator. The actuator is oriented so that it bends at the horizontal plane, therefore gravity does not affect the measurements. In our system setup not the elongation but the clamp can be moved on a circular trajectory to achieve a desirable curvature of the test sample.

The angle of the clamp is controlled via rotary solenoid actuator type GDRX-035. The voltage is applied to EAP through 1Ω resistor, and EAP current is calculated from resistor voltage drop. Input voltages for EAP and solenoid are input signals of the system. The Strain, current, and solenoid position are outputs of the system. Input signals are generated and outputs are measured using NI PCI-6036 data acquisition device connected to NI SC-2345 connector block. Inputs are controlled and outputs read by NI LabVIEW [22] program.

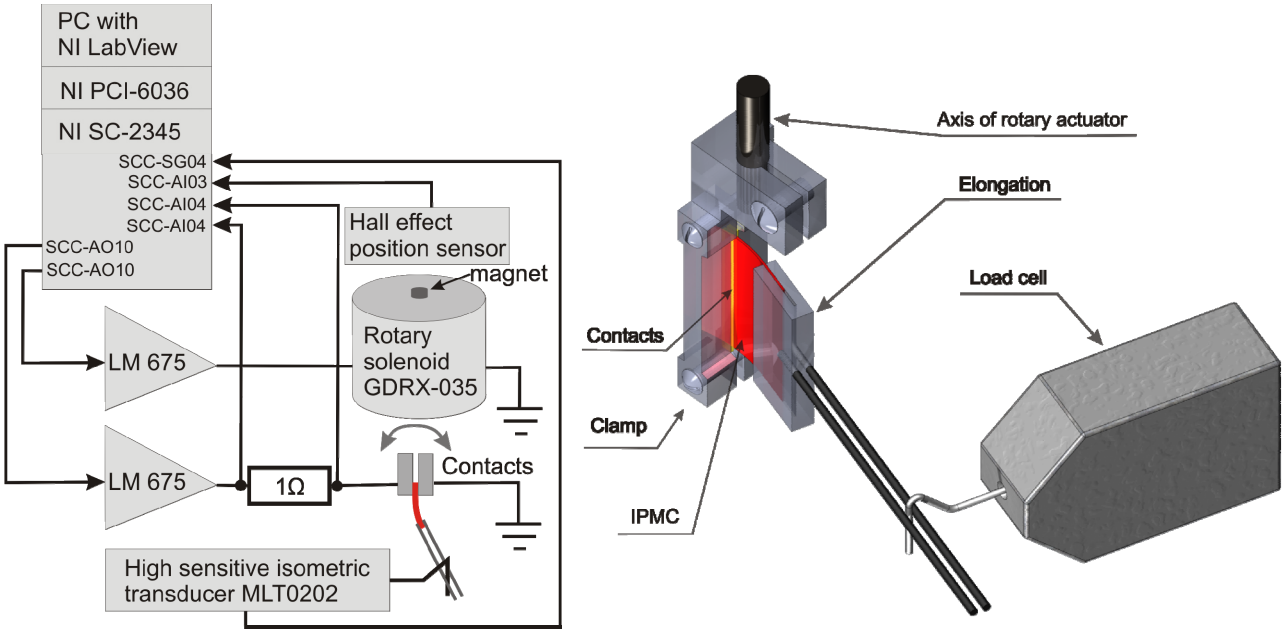


Fig. 3. The system setup. Diagram of the system setup (a) and close-up of the actuator (b).

A series of experiments can be generated in such a way that one or more parameters are variables. The system stabilizing and data acquisition minimum-time can also be specified. An average-cycle report is automatically generated after each test cycle.

## 4.2 The EAP material used in experiments

A type of ionic EAP called Ionomeric Polymer-Metal Composite (IPMC) was used in the experiments. The sample was purchased from Environmental Robots Inc.. Initially the sample was ionic-liquid based, but the solvent has been replaced by water. All experiments were performed with the same IPMC sheet, where the width of the IPMC sheet was $w = 19.0\,\text{mm}$, total length $l + l_c = 12.2\,\text{mm}$, and thickness $d = 0.28\,\text{mm}$.

The IPMC sample is plated with a thick platinum coating to minimize the effect of surface resistance.

In order to keep the hydration level constant, while avoid immersing the test instrumentation into the water, a recirculation water pump (windscreen washer pump) system was used to wet the test sample (see Fig. 4).

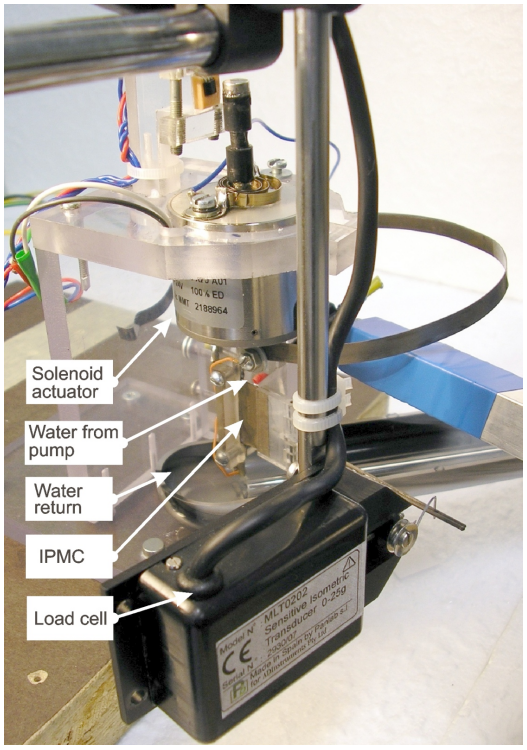


Fig. 4. Photo of the System setup. To keep the hydration level of IPMC constant water is pumped on it.

### 4.3 Measurement methodology

In this subsection the methodology used to identify the parameters of the material and the experiments to verify the model are discussed.

The parameters $\bar{K}$ and $\bar{Z}$ were determined by exciting the system with sinusoidal voltage input and measuring the output force and current. The amplitude of voltage was 1.6 V. The frequency of the input signal ranged from 0.037 Hz to 25 Hz. The angle of the actuator arm was maintained at 0.

Our experiments are mostly done in 0–20 Hz range where the viscoelasticity is not significant [15]. Therefore,we may only consider the static bending stiffness. It means that in our case the normalized bending stiffness is just a real-valued constant $\bar{B}(s) = \bar{B}$. The parameters $\bar{B}$ and $k_0$ were determined by measuring the output force of the actuator at two different deflection angles.

The experiments were carried out by varying free part and arm lengths. In case of each geometry also experiments at random voltages, angles, and frequency were performed. The total time consumed for the measurements in each geometry was about 40 minutes. All experiments were made at room temperature.

When the input signal starts, the system acquires a time to be stabilized. The stabilizing time on each $\bar{Z}$ and $\bar{K}$ measurement was 4 seconds or 1 period minimum, and measuring time was 6 seconds or 6 periods minimum. The stabilizing time on each random experiment was 15 seconds or 1 period minimum,and measuring time was 8 seconds or 8 periods minimum. The stabilizing time on each $\bar{B}$ and $k_0$ measurement was 10 seconds, and measuring time was 4 seconds.

## 5. RESULTS

Experiments were performed to characterize the material described in section 4.2 and to verify the model presented in section 3. Please see Table 2 for details about the different dimensions of the actuators used in series of experiments. Note that the experiments with the first set of dimensions of the actuator are repeated at the end. In each series normalized electromechanical coupling $\overline{K}$ and normalized electrical impedance $\overline{Z}$ were measured. Please see Fig. 5 for plots of measured average parameters $\overline{K}$, $\overline{Z}$ and standard deviation. The measured $\overline{K}$, $\overline{Z}$ are coherent with the results presented in [8].

In Fig. 6 the filtered averaged cycles of signals from 4.series are presented. The electrical model of IPMC is known to be nonlinear [23]. Our results also show that there is a notable nonlinearity in the electrical response at low frequencies..

Table 2. The geometries used in different series of experiments.

| Series | $l$ | $l_c$ | $w$ | $R$ |
|---|---|---|---|---|
| 1. | 6mm | 6.2mm | 19mm | 35mm |
| 2. | 6mm | 6.2mm | 19mm | 60mm |
| 3. | 8mm | 4.2mm | 19mm | 35mm |
| 4. | 8mm | 4.2mm | 19mm | 60mm |
| 5. | 6mm | 6.2mm | 19mm | 35mm |

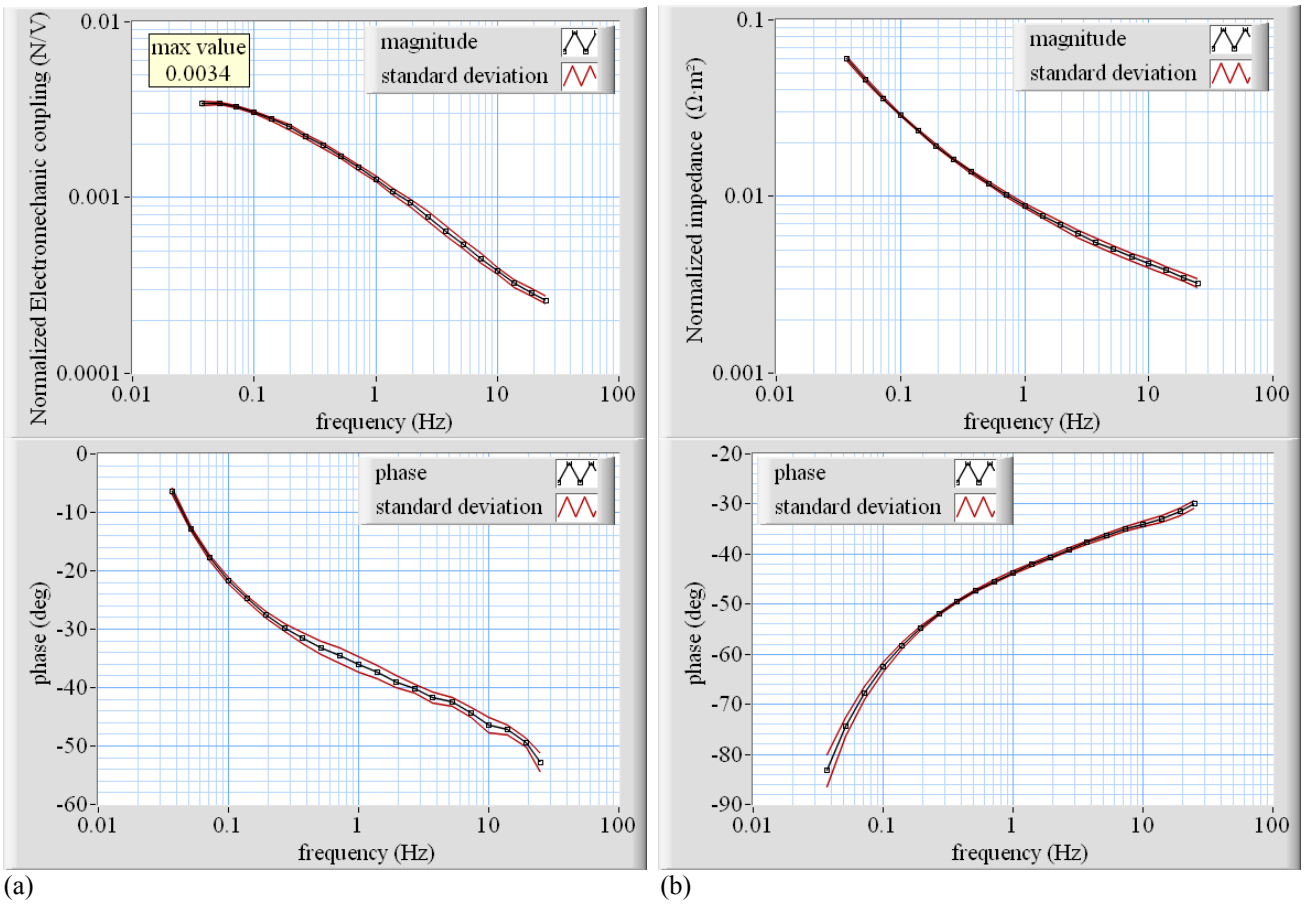


(a) (b)

Fig. 5. Plots of transfer functions a) normalized electromechanical coupling and b) normalized impedance.

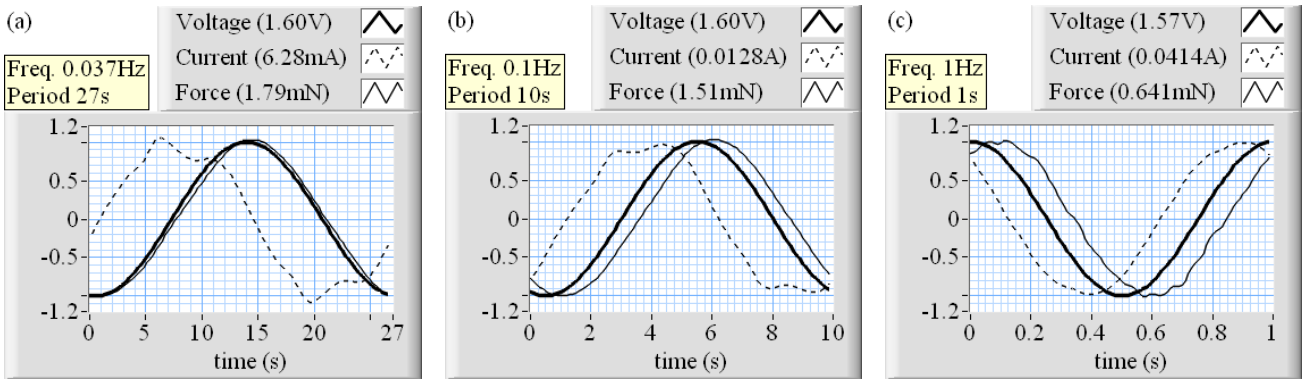


Fig. 6. Filtered averaged cycles of signals from 4. series.

In each series 24 experiments with random parameters were performed. The same set of randomly generated parameters was used each time to make results comparable. The limits of the parameters are given in Table 3. Before each experiment the parameters $\overline{B}$ and $k_0$ were measured – 24 times in each series. The normalized bending stiffness and the initial curvature measurements are presented in Fig. 7. Eventhough, the same IPMC piece was used for all the experiments in all series, $\overline{B}$ and $k_0$ vary notably.

The variation of the normalized bending moment can be explained by changes in the hydration process [24-27]. Using (2) from the mean normalized bending moment $\overline{B} = 0.71\,\mathrm{mN\cdot m}$ and thickness $d = 0.28\,\mathrm{mm}$, the equivalent Young modulus $E = 388\,\mathrm{MPa}$ can be calculated. This is in the range of other equivalent Young modulus for IPMC reported in the literature.

In Fig. 7 (b) initial curvature measurements are compared with angle amplitude before the measurements. There is a strong correlation between changes in the angle and in the initial curvature. This can be explained by the hysteresis in IPMC material [19-20].

Table 3. Limits of the parameters in random experiments.

| Parameter | Min | Max |
|---|---|---|
| Voltage – direct component | -0.01V | 0.2V |
| Voltage – alternating amplitude | 0V | 1.57V |
| Deflection angle – direct component | -15.1deg | 24.4deg |
| Deflection angle – alternating amplitude | 0 | 20.9deg |
| Frequency | 0.0607Hz | 27.8Hz |

The expected values for the random test outputs according to input signal parameters and previously measured material parameters were calculated on the basis of theoretical model and the result were compared to the measured output values. The difference of corresponding signals was expressed as relative deviation - root mean square deviation divided by mean root mean squares of signals. The relative deviation of the output force and current are presented in Fig. 8.

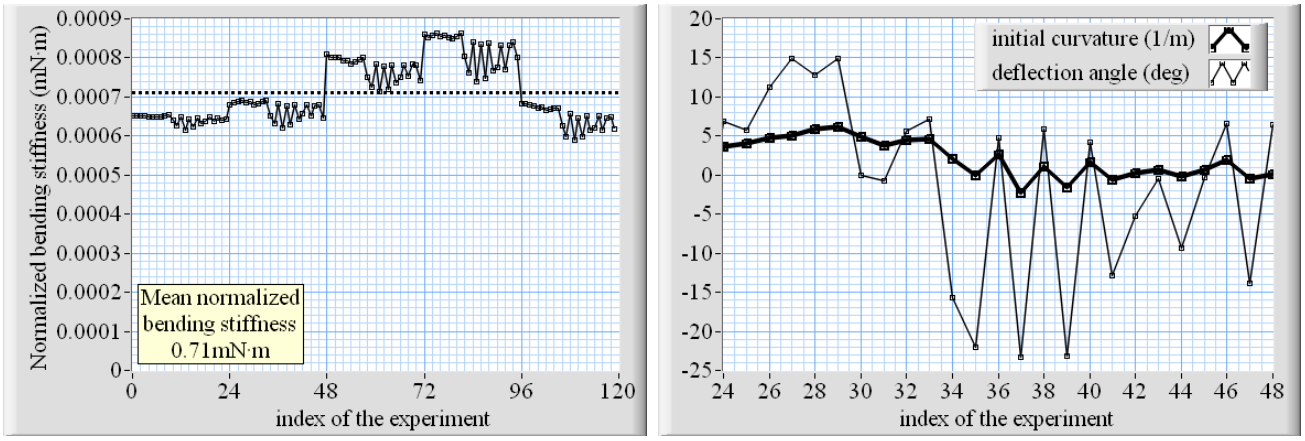


(a) (b)

Fig. 7. The normalized bending stiffness and initial curvature measurements. (a) normalized bending stiffness after experiments and (b) initial curvature after experiments.

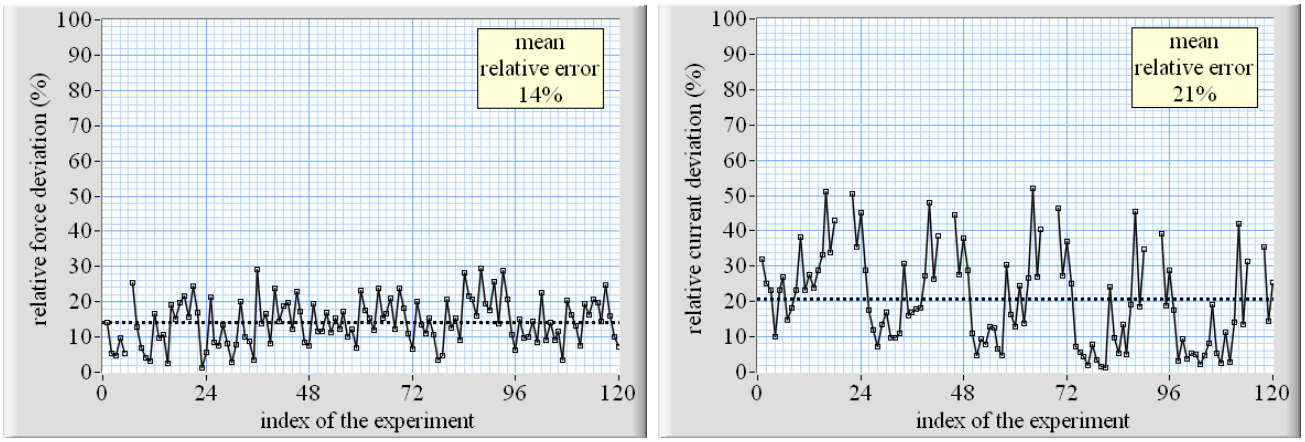


(a) (b)

Fig. 8. Relative deviation of (a) output force and (b) current.

## 6. CONCLUSIONS AND DISCUSSION

Actuators with different geometries were made using the same IPMC piece. For each geometry, parameters of the IPMC material were measured. The variation in the normalized electromechanical coupling and normalized electrical impedance were small. The normalized bending stiffness varied notably, but that can be explained with changes in the hydration level. The noticeable variation in the initial curvature can be explained by hysteresis in IPMC. Experiments with randomly selected parameters were conducted and the results were compared with the model prediction. Only a small difference was found. We conclude that the model proposed in this paper is scalable and valid.

The electromechanical response of some IPMC actuators is known to be in nonlinear [28]. However no nonlinearity was observed in electromechanical response of given IPMC sheet in the given frequency range. At the same time electrical response was notably nonlinear.

Bending EAP actuators are know for large deformations and linear models for well established feedback control techniques. Yet to the best of our knowledge no linear model for any bending EAP actuator that would enable large

deformations has been presented so far. In this paper such a model is presented and it is suitable for all bending EAP actuators. In addition the model considers dynamic behavior, initial curvature of EAP and enables concurrently varying load and position.

This model only holds when we consider all the parameters along the sheet to be approximately uniform. The bending moments generated along the sheet by outer force can be considered uniform only if $l \ll R$. Also in IPMC, the high resistance of the surface electrodes can cause the voltage distribution on the sheet to be non-uniform [8, 25, 29, 30]. The surface resistance also varies with curvature [31]. When the IPMC sheet is

1. sufficiently short,
2. surface conductivity is high enough, and
3. current is low enough,

electrically induced bending moment can be considered uniform along its length [11].

In the future for each type of EAP, the 4 empirical parameters should be modeled. At this stage, the normalized bending stiffness and initial curvature had to be measured before every experiment. It is also if the changes in  could modeled and estimated. For the future applications, if inertial forces need to be considered, corresponding terms should be added to model. Also electrical model should be improved to consider the nonlinearities. Many EAP actuators can be used as sensors. A similar model that was presented in this paper for EAP actuators should be derived for EAP sensors.

## ACKNOWLEDGEMENTS

The financial support by Tartu University Foundation and Estonian Science Foundation (grant #6765) is gratefully acknowledged. We would also like to thank Anoosheh Niavarani for reading the text and giving us suggestions.

## REFERENCES

[1] Bar-Cohen Y 2004 *Electroactive Polymer (EAP) Actuators as Artificial Muscles: Reality, Potential, and Challenges* (Bellingham, WA: SPIE Press)

[2] Mart Anton, Andres Punning, Alvo Aabloo, Madis Listak, Maarja Kruusmaa, "Towards a Biomimetic EAP Robot", in Proc. of TAROS 2004, "Towards Autonomous Systems Systems", University of Essex, 6.-8. Sept. 2004.

[3] A. Punning, M. Anton, M. Kruusmaa, A. Aabloo ,"A Biologically Inspired Ray-like Underwater Robot with Electroactive Polymer Pectoral Fins," IEEE Confrence "Mechatronics and Robotics 2004" (MechRob04); Aachen, Germany; 13.–15.09.2004. Aachen: Eysoldt, 2004, (2), 241–245.

[4] E. Mbemmo, Z. Chen, S. Shatara, X. Tan, "Modeling of Biomimetic Robotic Fish Propelled by An Ionic Polymer-Metal Composite Actuator," in *Proceedings of the 2008 IEEE International Conference on Robotics and Automation*, Pasadena, CA, pp. 689-694, 2008

[5] Chen Z, Shen Y, Xi N and Tan X 2007 Integrated sensing for ionic polymermetal composite actuators using PVDF thin films *Smart Mater. Struct.* 16 S262–71

[6] Bar-Cohen, Y., X. Bao, S. Sherrit, S. Lih, "Characterization of the electromechanical properties of Ionomeric Polymer-Metal Composite (IPMC)," *Proc. of SPIE*, v 4695, p 286–293, 2002.

[7] Diego Fernandez, Luis Moreno, and Juan Baselga, "Toward standardization of EAP actuators test procedures," *Proc. of SPIE* 5759, 274 (2005), DOI:10.1117/12.599106

[8] Z. Chen, X. Tan, "A Control-oriented and Physics-based Model for Ionic Polymer-Metal Composite Actuators," *IEEE/ASME Transactions on Mechatronics*, Vol. 13, No. 5, pp. 519-529, 2008

[9] Y. Fang, X. Tan, Y. Shen, N. Xi, G. Alici, "A Scalable Model for Trilayer Conjugated Polymer Actuators and Its Experimental Validation," *Materials Science and Engineering C: Biomimetic and Supramolecular Systems*, Vol. 28, pp. 421-428, 2008

[10] Bao X, Bar-Cohen Y, Chang Z and Sherrit, Stewart 2004 Characterization of bending EAP beam actuators Proc. SPIE Int. Soc. Opt. Eng. vol 5385 p 388–94
[11] Anton M, Aabloo A, Punning A and KruusmaaM 2008 A mechanical model of a non-uniform ionomeric polymer metal composite actuator *Smart Mater. Struct.* **17** 1–10
[12] Andres Hunt, Andres Punning, Mart Anton, Alvo Aabloo, and Maarja Kruusmaa, "A multilink manipulator with IPMC joints," *Proc. SPIE 6927*, 69271Z (2008)
[13] Seong-Hun Song, Kang-Min Park, Woo-Sik Kim, Sang-Mok Chang, Analysis of the characteristics of electrochemically polymerized polypyrrole films by using QCA and AFM, Materials Science and Engineering: C, Volume 24, Issues 1-2, 14th Molecular Electronics and Devices Symposium, 5 January 2004, Pages 225-227, ISSN 0928-4931, DOI: 10.1016/j.msec.2003.09.066.
[14] Newbury K and Leo D J 2003 Linear electromechanical model of ionic polymer transducers—part I: model development *J. Intell. Mater. Syst. Struct.* **14** 333–42
[15] Newbury K and Leo D J 2003 Linear electromechanical model of ionic polymer transducers—part II: experimental validation *J. Intell. Mater. Syst. Struct.* **14** 343–57
[16] Gursel Alici, Brian Mui, Chris Cook, Bending modeling and its experimental verification for conducting polymer actuators dedicated to manipulation applications, Sensors and Actuators A: Physical, Volume 126, Issue 2, 14 February 2006, Pages 396-404, ISSN 0924-4247, DOI: 10.1016/j.sna.2005.10.020.
[17] Choonghee Jo, Hani E Naguib and Roy H Kwon, "Modeling and optimization of the electromechanical behavior of an ionic polymer–metal composite," Smart Materials and Structures, Vol. 17, pp. 065022 (13pp), December 2008
[18] J. Carmeliet and K. Van Den Abeele, "Mesoscopic approach for modeling the nonlinear hysteretic response of damaged porous media in quasi-static and dynamic loading: Effects of pressure and moisture saturation," in *Proceedings of the 4th International Conference on Fracture Mechanics of Concrete and Concrete Structures*, 2001.
[19] Z. Chen, X. Tan, M. Shahinpoor, "Quasi-static Positioning of Ionic Polymer-Metal Composite (IPMC) Actuators," *Proceedings of the IEEE/ASME International Conference on Advanced Intelligent Mechatronics*, Monterey, CA, pp. 60-65, 2005
[20] Chul-Jin Kim, Hyun Woo Hwang, No-Cheol Park, Hyun-Seok Yang, Young-Pil Park, Kang-Ho Park, Hyung-Kun Lee, and Nak-Jin Choi "Preisach modeling of IPMC-EMIM actuator" Proc. SPIE 6927, 692725 (2008)
[21] Mart Anton, PhD thesis "Mechanical modeling of IPMC actuators at large deformations" [supervisors: Maarja Kruusmaa, Alvo Aabloo, Jan Villemson ; Faculty of Mathematics and Computer Science, University of Tartu, Estonia] Tartu : Tartu University Press, c2008, 123 p
[22] http://www.ni.com/labview/
[23] Bonomo C, Fortuna L, Giannone P, Graziani S and Strazzeri S 2007 A nonlinear model for ionic polymer metal composites as actuators *Smart Mater. Struct.* 16 1–12
[24] Characterization and dynamic modeling of ionic polymer-metal composites (IPMC): artificial muscles Ashwin Mudigonda and Jianchao J. Zhu Proc. SPIE 6168, 616815 (2006)
[25] Nemat-Nasser S andWu Y 2003 Comparative experimental study of ionic polymer–metal composites with different backbone ionomers and in various cation forms *J. Appl. Phys.* **93** 5255–67
[26] Newbury K 2002 Characterization, modeling, and control of ionic polymer transducers *Dissertation* Virginia Polytechnic Institute and State University
[27] Porfiri, M., 2009: "An electromechanical model for sensing and actuation of ionic polymer metal composites", *Smart Materials and Structures*, 18(1), 015016
[28] C. Kothera, Characterization, Modeling, and Control of the Nonlinear Actuation Response of Ionic Polymer Transducers. PhD thesis, Virginia Polytechnic Institute and State University, September 2005.
[29] Punning A, KruusmaaM and Aabloo A 2006 Surface resistance experiments with IPMC sensors and actuators *Sensors Actuators* A **133** 200–9
[30] Shahinpoor M and Kim J K 2000 The effect of surface-electrode resistance on the performance of ionic polymer–metal composite (IPMC) artificial muscles *Smart Mater. Struct.* **9** 543–51
[31] Punning A, Anton M, Kruusmaa M and Aabloo A 2006 Empirical model of a bending IPMC actuator *Proc. SPIE* 6168 61681V